Multifractal analysis application to the study of fat and its infiltration in Iberian ham: influence of racial and feeding factors and type of slicing

S. Serrano[a*], F. Perán[a], E. Gutiérrez de Ravé[b], A. Cumplido[a] and F.J. Jiménez-Hornero[b]

[a] Department of Food Hygiene and Technology. University of Cordoba. Campus Rabanales, Edif. Darwin, anexo. Cordoba. 14071. Spain

[b] Department of Graphic Engineering. University of Cordoba. Campus Rabanales, Edif. Mendel. Córdoba. 14071. Spain

[*] Corresponding author: Salud Serrano. Department of Food Hygiene and Technology. University of Cordoba. Campus Rabanales, Edif. Darwin, anexo. Cordoba. 14071. Spain. Tel. +34957212654. Fax +34957212000. E-mail: bt2sejis@uco.es

Abstract

This paper explores the multifractal features of different commercial designations of Iberian ham (acorn 100% Iberian ham, acorn Iberian ham, feed/pasture Iberian ham and feed Iberian ham). This study has been done by taking as input the fatty infiltration patterns obtained from digital image analysis of ham cuts comparing mechanic and manual slicing. The yielded results show the multifractal nature of fatty connective tissue in Iberian ham, only when knife cutting is applied, confirming the differences between the designations according to their genetics and feeding. Thus, the multifractal parameters presented in this work could be considered as additional information for checking Iberian ham quality by using non-destructive methods based on the combination of image analysis and predictive techniques. Meat industry can take advantage of these methods to evaluate meat products, especially when fat-connective tissue with complex pattern distribution is involved.

Keywords: Iberian ham; fatty infiltration; manual slicing; machine slicing; image analysis; multifractal analysis.

1. Introduction

1.1 The fatty infiltration in the Iberian Pig

The Iberian pig refers to a racial group derived from the Mediterranean archaic pig (*Sus mediterraneus* or southern *Sus scrofa*). This pig is located on southern and central areas of the Iberian Peninsula. The main benefit of this breed has its origin in its adaptation to the ecosystem. The quality of the Iberian pig products is based on genetic features (breed), nutrition and food processing (Fernandez, Monin, Talmant, Mourot, & Lebret, 1999). According to the type of nutrition, the Iberian pig products designations will depend on the amount of acorn in their diet (called "Montanera").

Referred to the process of elaboration, the peculiar characteristics of the Iberian ham are closely linked with climatic and human process factors (in the know how to be transmitted between generations) that occur in several localities of the South-East of the Iberian Peninsula (Ventanas, 2008) and that have achieved just fame for the quality of their products. The different conditions (salt, moisture, temperature, time) that occur in the different stages of the process and in the hams produced in different geographic locations modify the course of ripening reactions and, consequently, the balance of the flavours and aromatic compounds of the product. This fact justifies the existence of several Protected Designations of Origin (PDO).

Another fundamental quality factor of the product is the long maturation period (about 2 years). The development of the aroma reactions is very slow, since the end products of many of them are the substrates of others that take place later. Only very late in the process occur dry conditions (low water activity) and increase in temperature allowing the formation of compounds capable of triggering the perception of characteristic aroma. Both the intensity and presentation of the aroma, as well as some specific aroma attributes (cured, nuts, etc.) and some less rancidity resent if the 9-12 months of maturation marked by the PDOs are not respected.

The greatest characteristic of Pure Iberian pigs is the specific way of fat distribution (Serrano, Perán, Jiménez-Hornero & Gutiérrez de Ravé, 2013). The ability to infiltrate fat between muscle fibres is a feature of this race. This pattern of fat distribution is different between Iberian pigs and crossbred pigs (Morcuende, Estévez, Ramírez, de Alba, & Cava, 2003; Tejada, Gandemer, & Antequera, 2002; Fernández, de Pedro, Núñez, Silio, García-Casco, & Rodríguez, 2003).

Genetics and type of feed cause modifications in the fat, and particularly in the fat that we eat with the meat or with the ham; Which directly or indirectly determines both the nutritional-dietary aspects and most of the sensorial characteristics we perceive. In fresh meat as in products of the Iberian pig (loins and hams), the quantity, composition and structure of the intramuscular fat are decisive for the attributes of appearance, texture, and aroma, as well as for the type of processing, conditions, and duration (Ventanas, 2008). The higher intramuscular fat content in the muscles of the Iberian pig represents a fundamental aspect for the higher quality of their meat with respect to the white races selected to produce meat and slaughtered at 4-6 months of age. The abundant intramuscular fat has clear effects on the palatability of the meat: on the one hand it decreases the cutting force during chewing, facilitating the separation of the muscular fibres and improving the sensation of tenderness of the meat.

1.2 Authenticity of breed

Under current legislation, they are designation of 100% Iberian and Iberian designation that allows 50% Duroc´s genome. Farmers are required to the registration of their animals by means of a certification body that guarantees the breed purity (Real Decreto 4/2014). The genetic testing is used if suspicions of paternity exist, but it is an expensive and laborious analysis. Several analytical techniques have been used with the aim to authenticate the Iberian pig´s fat (Casillas, 1994) or muscle. These technics include analysis of (i) stable isotopes and muscle by using electronic olfactometry subcutaneous fat proposed by González-Martín, González-Pérez, Hernández-Méndez, Marqués-Macías, and Sanz-Poveda (1999) and González-Martín, González-Pérez, Hernández-Méndez, Marqués-Macías, and Álvarez-García (2000), (ii) the Near Infrared Spectroscopy technique for the determination of fatty acids (García, 2002), and (iii) the determination of triglyceride content and compounds present in the unsaponifiable fraction of the fat (Ruiz, & Petron, 2000), without any have given definitive results. The use of feed enriched in oleic acid in many cases makes it difficult or impossible to correctly classify the raw material according to the feed received by the pigs, based exclusively on the fatty acid analysis of the subcutaneous fat.

1.3 Overview of multifractals and digital image analysis in food science

The fractal concept was proposed by Mandelbrot (1982). Fractal objects have the property of self-similarity (i.e. the geometrical or topological properties are invariant at different scales), and they are characterized by a non-integer (fractal) dimension 'between' the conventional Euclidean dimensions of 1, 2 and 3. However, there are cases where the fractal object exhibits different exponents under different scales. Those are called multifractals being characterized by a sequence of fractal dimensions that establishes the local variance of the geometrical properties under scale changes. It is assumed that these structures are composed by different fractals coexisting on the same support. The self-similarity can be described by the generalized fractal dimensions spectrum that establishes the specific fractal behavior of the set at a given scale. According to Baravalle, Delrieux, and Gómez (2015), who performed a categorization of bread crumb structure, the multifractal approach is suitable to perform food classification since variations in local regions are captured in an accurate manner. In this sense, previous works such as Serrano et al. (2013) demonstrated how some multifractal descriptors (i.e. particular fractal dimensions) were suitable to describe fatty infiltration in Iberian and White pork sirloins. Both mentioned works are some samples of the benefits obtained, over the last two decades, by using fractal/multifractal approach to qualitatively characterize food morphology because the highly irregular structures of many food materials elude precise quantification by conventional means. Food with a complex geometry in which a large category of structural irregularities exists, including pores, protuberances, and apparently replicating structures is not easy to characterize. In this situation fractal/multifractal parameters can be regarded as suitable descriptors of food structure. Thus, recent works are focused in the application of the multifractal framework to describe food structure. It can find relevant examples in the literature such as Mendoza, Verboven, Ho, Kerckhofs, Wevers, and Nicolaï (2010) and Mendoza, Valous, Delgado, and Sun (2011), who characterize apple pore and ham fat-connective tissue size distributions, García-Armenta et al. (2016) for describing breakage patterns of tortilla chips, Cáez-Ramírez, Alamilla-Beltrán, and Gutiérrez-López (2017) who evaluated senescence advance in fresh-cut papaya and Jung and Yoon (2017), to determine the influence of relative humidity on the rupture patterns of dried marine algae.

In the referred works above, digital food image analysis (DFIA) plays a main role. There is diversity of techniques applied to DFIA, which is capable of extracting various features such as colour, texture, shape, and size (Zheng, Sun, & Zheng, 2006; Kaya, Ko & Gunasekaran, 2008; Kumar, & Mittal, 2010; Fathi, Mohebbi, & Razavi, 2009). These simple appearance features have allowed task-relevant analysis and interpretation with precision, objectivity and speed in the quality grading and classification of many foods (Hutchings, Luo, & Ji, 2002). Consequently, they could also be used for the automation of meat products inspection and quality grading (Valous, Mendoza, Sun & Allen, 2009a, 2009b; Romano, Masi, & Cavella, 2018). DFIA techniques can perform objective measurements of features related to the visual appearance and textural patterns not detected by human vision. In meat and meat products, the fat-connective tissue (FCT) size distribution represents a fundamental physical property used for quality assessment purposes. Recently, Serrano et al. (2013) applied the blend of DFIA and multifractal analysis as a non-destructive procedure to check quality in some meat pieces (i.e. pork sirloin) which exhibit very variable FCT.

The general objective of this paper is to explore the multifractal nature of the FCT distributions present in samples of Iberian ham designations (acorn 100% Iberian ham, acorn Iberian ham, feed/pasture Iberian ham and feed Iberian ham) obtained by using knife and slicer cutting. For this purpose, after performing a DFIA of the samples, the relationship between some multifractal descriptors and FCT spatial pattern was investigated.

2. Material and methods

2.1 Ham samples

Four Iberian ham designations according to Real Decreto 4/2014 were studied in this work. A brief description of them is given below:

Acorn 100 % Iberian Ham (A100IH): the piece is obtained from pigs whose progenitors, mother and father, are breeding pure Iberian pigs and they are slaughtered immediately after the feeding with acorns, grass and other natural resources, exclusively.

Acorn Iberian Ham (AIH): the piece is obtained as of pigs from crossing of breeding pigs: Iberian (100%) female and Duroc male as normative requisites, they are slaughtered immediately after the feeding with acorns, grass and other natural resources, exclusively.

Feed/Pasture Iberian Ham (FPIH): the piece is obtained as of pigs from crossing of breeding pigs: Iberian (100%) female and Duroc male as normative requisites, and after of a minimum of weigh with acorn their feeding is completed with cereal and leguminous feed till slaughtered, in extensive farming.

Feed Iberian Ham (FIH): the piece is obtained as of pigs from crossing of breeding pigs: Iberian (100%) female and Duroc male as normative requisites, and their feeding is with cereal and leguminous feed till slaughtered, in intensive farming.

Regarding to the Iberian ham samples analysed in this research, Livestock Breeders Cooperative “COVAP” provided 32 vacuum packs (with 12 slices each one) that were grouped into 4 sets (consisting of 8 packs each one) according to the four ham designations mentioned before. Thus, the configuration of each set corresponded to 4 packs containing slices obtained from manual cutting with knife and 4 packs including slices cut with machine. Half sample (6 slices per pack) was used for laboratorial determinations (total fat, moisture and water activity), which were made in duplicate, and the other half (6 slices per pack) for image and multifractal analyses.

Finally, it must be mentioned that commercial brand informed each pack came from a unique ham to follow its traceability

2.2 Physicho-chemical determinations

Water activity (a_w) was determined with Novasina® apparatus IC-500 AW-LAB (Swiss). Water content was obtained by desiccation till constant weight according to AOAC method (1980). Total fat was determined using AOAC method number 960.39 (1980). It was realized the variance analysis (ANOVA) using SPSS 13 software.

2.3 Image acquisition and processing

The method proposed by Serrano et al. (2013) was followed here. The system for obtaining images consists of (i) light source (four panels with four white fluorescent light tubes of 36 W, 5400 K colour temperature), (ii) digital camera (Nikon D60 with 18-55 mm lens, fixed on a tripod structure vertically adjustable) connected via a USB cable to a personal computer, and (iii) imaging software (Adobe Photoshop CS3 10.0). The system took standardized images (3872x2592 pixels with fine quality in JPEG format) by manually setting the following parameters: 36mm zoom, focal distance 26mm, shutter speed 1/60 seconds, aperture of f/8, ISO 200, no flash and fit the white balance using a grey card with 18% reflectance. It was obtained one colour image from each slice included in a vacuum pack which was transformed into white (pixels occupied by fat) and black (pixels of lean meat) image by setting a threshold in 175. Afterwards, a square of 512x512 pixel was extracted as region of interest (ROI) from all the black and white images. The dimension of this ROI, power of 2 for computational purposes, was determined as the largest length that fits in all of these ham images ensuring, at the same time, locations far from the edges to avoid potential border effects on the results and optimizing the coefficients of determination r2 of the fits involved in the multifractal analysis introduced in the next section (Mendoza, Valous, Sun & Allen, 2009). Consequently, the ROI position varied from one ham slice image to another. The new high-quality JPEG image was used to perform the multifractal analysis. With this aim, this image was transformed into a data file with a structure in three columns by using a toolbox of Matlab (MathWorks, Inc., USA). The first two columns referred to the position of each pixel and the third contained colour code (1: for white fat, 0: colour black refers to lean meat). This data file was stored in text format (TXT). Fig. 1 shows an example of the initial image of the sample and the squared black and white ROI.

2.4 Multifractal sandbox method

The fixed-size box-covering algorithm (Halsey, Jensen, Kadanoff, Procaccia, & Shraiman, 1986) is widely used for multifractal analysis. According to De Bartolo, Gaudio, and Gabriele (2004), two methods can be applied with this algorithm: i) box-counting (i.e. Block et al., 1990), in which a grid of size R is used; ii) sandbox (Tél, Fülöp, & Vicsek, 1989; Vicsek, 1990; Vicsek, Family, & Meakin, 1990), in which regions of size R are chosen around randomly selected points on the fractal set contained in the ROI. The presence of areas containing few data points, as it happens in the ham FCT distribution, is the principal cause of the biased assessment of the generalized fractal dimensions for negative probability moment orders, q, in the box-counting method (i.e. De Bartolo et al., 2004; Dómbradi, Timár, Bada, Cloetingh, & Horváth, 2007). As the sandbox method overcomes this drawback, it has been selected to perform the multifractal analysis in this work.

The sandbox approach considers the amount of fat pixels in the ROI, M(R), within circles of given radius R. Each one of those circles is centered on a pixel occupied by fat which is randomly chosen. With this aim, the random number generator of Park and Miller combined with a Marsaglia shift (Press, Teukolsky, Vetterling, & Flannery, 1996) was applied. According to Tél et al. (1989), the generalized fractal dimension, D_q, of moment order q is determined by:

$$D_q(R/L) = \frac{1}{q-1} \lim_{R/L \to 0} \frac{\ln\left\langle \left[M(R)/M_0\right]^{q-1} \right\rangle}{\ln(R/L)}, \text{ for } q \neq 1 \tag{1}$$

Where M_0 is the total number of fat pixels in the ROI and L stands for the normalized image dimension. The brackets ⟨⟩ mean to take statistical average over randomly chosen centers of the circles.

When $q = 1$, the solution for D_q is yielded through the Taylor's expansion around $1+dq$ (e.g. De Bartolo et al., 2004)

$$D_1(R/L) = \lim_{R/L \to 0} \frac{\left\langle \ln\left[M(R)/M_0\right] \right\rangle}{\ln(R/L)} \tag{2}$$

Generalized dimensions can be found through the linear fit slope of the scaling curves $\ln\langle[M(R)/M_0]^{q-1}\rangle$ versus $\ln(R/L)$ for $q \neq 1$ and $\langle\ln[M(R)/M_0]\rangle$ versus $\ln(R/L)$, for $q = 1$. Linear fit is performed by considering $(R/L)_{lower}$ and $(R/L)_{upper}$ as the low and high limits.

Following Grassberger (1983) and Grassberger, and Procaccia (1983), D_q is a decreasing function with respect to q for a measure multifractally distributed. Among the fractal dimensions, those denoted as D_0, D_1 and D_2 are frequently used to extract information from image analysis results. A brief description of these parameters is given in the next lines. Thus, D_0 is the the box-counting dimension (or fractal dimension of the set over which the measure is carried out. It describes how the geometric pattern covers the domain but is not sensitive to density distribution. D_1 is the information or entropy dimension being related to the uniformity in the measure distribution (i.e. density of the fractal points). D_2 is the correlation dimension and indicates the correlation between two points of the fractal (i.e. pattern complexity).

3. Results and discussion

3.1 Physicho-chemical parameters

Table 1 shows results for total fat, moisture and water activity (a_w). The obtained results differ from authors such as Ventanas (2008), who states that Iberian ham does not have a high fat content in spite of appearances and, thus, pure Iberian hams from “Montanera”, which are the ones with the highest infiltration, usually contain 8-10% infiltrated fat and, depending on the area of the ham and the type of cut, an additional 5-9% of subcutaneous and intermuscular fat. Faced with this range of 13-19%, this work obtains a range of 20-42% for A100IH and 18-49% for FPIH However, the mean total fat obtained for AIH coincides with Cabezas, Galán and Fernández-Salguero (2012), that obtain a value of 35.32%.

The statistical analysis of the results of total fat, humidity and water activity did not obtain significant differences between the four groups of samples.

3.2 Multifractal analysis

The pixels of the processed images (knife and slicer cutting) belonging to the ham fat-connective tissue (FCT) were considered when performing the multifractal analysis. Thus, M_0 was the total amount of these pixels and $M(R)$ was the quantity of them falling in a circle of given normalized radius R. One hundred values R, equally distributed for $(R/L) \in [0.015, 0.25]$, were considered in the calculations with the aim of keeping $R<<L$, $L = 1$ being the normalized ROI dimension. This selection ensures accuracy when using the sandbox method (e.g. De Bartolo et al., 2004; Dómbradi et al., 2007). For each radius, the number of circles, nc, whose centres were randomly located on the FCT, was determined by L/R. The scaling curves found look alike Fig. 2a in all the cases. These

curves were obtained for selected values of $q \in [-5, 5]$. Lower and upper cuts, $(R/L)_{lower} = 0.05 \pm 0.0035$ and $(R/L)_{upper} = 0.18 \pm 0.03$, maximised the goodness of the fits got by applying the least squares linear regression between them to determine the generalized fractal dimensions D_q as the slope of the linear part of these plots (see Fig. 2a). The coefficient of determination yielded, r^2, was higher than 0.995 in all the cases. Figure 2b shows a sample of the spectrum of the generalized fractal dimensions obtained with the sandbox method. For the different Iberian ham designations, D_q was a decreasing function resembling Fig. 2b, with $D_0 > D_1 > D_2$ denoting a multiscaling behaviour.

According to the yielded results, the four designations of Iberian ham fat-connective tissue exhibits a multifractal nature. So, the next step was to apply the multifractal framework to describe different kinds of Iberian ham. With this aim, the same four parameters tested by Serrano et al. (2013) derived from the generalized dimensions spectra, were considered here: D_0, D_1, $D_0 - D_1$ and D_2.

Tables 2 and 3 list the fractal dimensions mean values and their standard errors obtained when knife and slicer cutting is considered. Multifractal nature is present in all the ham designation because $D_0 > D_1 > D_2$. There are not rules to set the acceptable standard error values when determining fractal dimensions (Benguigui, Czamanski, Marinov & Portugali, 2000). Although those found in this work are relatively high, they are suitable because all of them are lower than 0.1 (Chen, Wang & Feng, 2017). Each fractal dimension exhibits a clear ascending or descending trend following the order A100IH, AIH, FPIH and FIH for knife cutting (Table 2). This situation is not found in Table 3 for slicer cutting. In addition, similar mean values are listed for each fractal dimension in the same table, except for A100IH designation. Therefore, the multifractal description of ham designations is limited when the slicer cutting is used. Figures 3 to 6 show the relationships between these fractal dimensions and fat fraction (ratio between FCT pixels and the total amount image pixels) for the Iberian ham designations considered here. In the same figures, the data are grouped according to the kind of cutting performed. According to Figs. 3a, 4a, 5a and 6a there is a clear relationship between the multifractal parameters and fat fraction when the knife cutting is used. As it can be appreciated, this circumstance is evident for A100IH and FIH designations, which are in separated areas of the plots shown in these figures. When AIH and FPIH designations are considered, the situation described before is not so evident because there is some mixing of their points. However, the areas occupied in the plots by AIH and FPIH designations are always next to the places where A100IH and FIH, respectively, are. The tendency described above was not found for ham designation from samples cut with slicer. Figures 3b, 4b, 5b and 6b show that there are not specific locations for the ham designations in the plots. By contrast, the points are mixed in a narrow range for fat fraction values (≤ 0.3) in all the cases. It must be noted that the same fat fraction is the boundary between the areas where A100IH and FIH designations data are placed in Figs. 3a, 4a, 5a and 6a. Thus, it can be inferred again that the multifractal discrimination of ham designations is not suitable when the slicer cutting is considered. However, it should be noted that the fat fraction dismisses, compared to knife cutting, mainly affects to AIH, FPIH and FIH designations showing similar values (0.1-0.25) for A100IH ham in both cases.

Focusing on the revealed relationships between fractal dimensions and fat fraction for the knife cutting cases, it can be seen in Fig. 3a that A100IH has higher values for D_0 than FIH designation. It means that A100IH needs less fat fraction to fill the slice surface than FIH suggesting different geometric distributions for the FCTs. Nevertheless, AIH and FPIH designations exhibit similar FCT slice covering according to the values obtained for D_0. However, this fractal dimension does not properly describe the FCT density distribution because similar D_0 values might correspond to completely different FCT physical layouts. For this reason, it is advisable to consider D_1 and D_2 dimension. Figure 4a shows the yielded fractal information dimensions, D_1. As it can be checked, except for A100IH, the ham designations exhibit similar values for this parameter. Therefore, it is not possible to describe the FCT density distribution considering D_1 alone. With the aim of overcoming this drawback, $D_0 - D_1$ were used because lower this parameter higher uniformity in FCT density distribution. Figure 5a shows the $D_0 - D_1$ values corresponding to each ham designations. A100IH has the highest records for this parameter meaning that its FCT density distribution is less uniform than the rest of the designations. In the same figure, it can be appreciated decreasing values for $D_0 - D_1$ according to the order AIH, FPIH and FIH. This fact evidences that the FCT density distribution is more uniform in these ham designations as the fat fraction increases. Finally, Fig. 6a show the relationships between FCT fractal correlation dimension and fat fraction. The lower D_2 values are displayed for A100IH designation implying that its FCT distribution shows the lesser complex pattern. This complexity grows as D_2 increases for AIH, FPIH and FIH, by order, denoting a direct relationship to fat fraction.

Figures 7 and 8 depict the statistical distributions found for the fractal dimensions mentioned above (knife cutting case) by taking into account an interquartile range affected by a factor of 1.5 to determine whisker lengths and outliers. As it can be checked in Fig. 7, D_0 and D_1 considered as independent parameters do not provided any relevant information on ham designation. However, Fig. 8 shows significant differences for A100IH statistical distribution $D_0 - D_1$ compared to the rest of designations. The same fact occurs when D_2 is considered. According to the reported results, the combined use of $D_0 - D_1$ and D_2 provides a description of the FCT distribution for Iberian ham designations, especially A100IH and FIH.

There is a growing trend in the prediction of food quality based on the joint application of DFIA and data mining and machine learning (i.e. Ropodi, Panagou, & Nychas, 2016). Both techniques can be considered as non-destructive methods for the characterization of the composition of raw materials and end-products. They are recent examples of this growing trend that overcomes the drawbacks of the sensory analyses (i.e. destructive, time-consuming, costly, sample preparation, as Valous, Zheng, Sun, and Tan, 2016, stated). Data mining is an iterative process of creating a predictive and descriptive model, by detecting unidentified patterns in vast amounts of data to support decision making. It has been applied to determine sensory parameters in Iberian ham (Pérez-Palacios, Caballero, Caro, Rodríguez, & Antequera, 2014; Caballero et al., 2016) and loin (Pérez-Pérez-Palacios, Caballero, Antequera, Durán, Ávila, & Caro, 2017; Caballero et al., 2017; 2018). By other hand, machine learning refers to an algorithm that improves automatically through experience based on data. Random forest (Breiman, 2001) is one of the most used algorithms, among the available ones for this technique, to categorize food. Thus, Liu, Wang, Wang, and Li (2013) applied it to the recognition of orange beverage and Chinese vinegar, Ai et al. (2014) to select premium quality vegetable oils, Barbon et al. (2016, 2017) to predict storage time prediction of pork meat and to evaluate marbling meat, respectively, and Santos Pereira, Barbon, Valous, and Barbin (2018) to forecast the ripening of papaya fruit. In all the cases, databases containing features obtained from computer vision techniques were required to perform the studies. However, fractal parameters were included in these databases few times. In this sense, it has to be remarked that Caballero et al. (2017; 2018) shown the higher accuracy in the prediction of pork meat quality when they were included in the studies. As it has been demonstrated by Serrano et al. (2013) for Iberian pork sirloin and here, for Iberian ham, the distribution of the FCT exhibits a multifractal nature described by fractal dimensions $D_0 - D_1$ and D_2. As a consequence, these multifractal metrics can be seen as supplementary features of those considered in the databases extracted from DFIA and used to foresee pork meat quality.

4. Conclusions

Digital food image analysis and sandbox method have been used here to perform a multifractal study of the fat infiltration in Iberian ham. The found results show the multiscaling behavior of the fat infiltration in Iberian ham. However, the results yielded from the multifractal analysis applied in this work are only useful to depict ham designations when knife cutting is applied. The investigation carried out in this work demonstrates that capacity and information fractal dimensions, through the values yielded for $D_0 - D_1$, and the correlation fractal dimension D_2 can be regarded as features linked to ham quality. This situation is not so evident when machine cutting is performed. The knife cut is done following the direction of the muscle fibers while machine cutting is usually made perpendicular to these fibers altering the distribution pattern of fatty infiltration. In fact, multifractal analysis results suggest some uniformity in the resulting patterns of applying this type of cut, with independence of the ham designation considered.

The use of non-destructive methods to predict meat quality is essential for the involved industry to overcome the difficulty of making standardization and control tasks due to the presence of highly variable fat-connective tissue. The findings reported in this work give the chance of including the metrics derived from the multifractal analysis as features in the databases used by data mining and machine learning to improve the results of these predictive techniques.

5. Acknowledgements

The authors gratefully acknowledge the support of the Andalusian Research Plan Groups TEP-957 and AGR-202. The authors wish to express their appreciation to the Livestock Breeders Cooperative “COVAP” (Córdoba, Spain) for their collaboration in providing the samples.

6. References

Ai, F., Bin, J., Zhang, Z., Huang, J., Wang, J., Liang, Y., … Yang, Z. (2014). Application of random forests to select premium quality vegetable oils by their fatty acid composition. *Food Chemistry*, *143*, 472–478.

AOAC (1980). *Official Methods of Analysis*. (13th ed.). Washington, D.C: Association of Official Analytical Chemists.

Baravalle, R. G., Delrieux, C. A., & Gómez, J. C. (2015). Multifractal characterisation and classification of bread crumb digital images. *Journal on Image and Video Processing*, *9*.

Barbon, A. P. A. C., Barbon, S., Mantovani, R. G., Fuzyi, E. M., Peres, L. M., & Bridi, A. M. (2016). Storage time prediction of pork by Computational Intelligence. *Computers and Electronics in Agriculture*, *127*, 368–375.

Barbon, A. P. A. da C., Barbon, S., Campos, G. F. C., Seixas, J. L., Peres, L. M., Mastelini, S. M., … Bridi, A. M. (2017). Development of a flexible Computer Vision System for marbling classification. *Computers and Electronics in Agriculture*, *142*, 536–544.

Benguigui, L., Czamanski, D., Marinov, M., & Portugali, Y. (2000). When and Where is a City Fractal? *Environment and Planning B: Planning and Design*, *27*, 507-519.

Block, A., von Bloh, W., & Schellnhuber, H. J. (1990). Efficient box-counting determination of generalized fractal dimensions. *Physical Review A*, *42*, 1869-1874.

Breiman, L. (2001). Random forests. *Machine Learning*, *45*, 5–32.

Caballero, D., Antequera, T., Caro, A., Amigo, J. M., ErsbØll, B. K., Dahl, A. B., & Pérez-Palacios, T. (2018). Analysis of MRI by fractals for prediction of sensory attributes: A case study in loin. *Journal of Food Engineering*, *227*, 1–10.

Caballero, D., Caro, A., Rodríguez, P. G., Durán, M. L., Ávila, M. del M., Palacios, R., Pérez-Palacios, T. (2016). Modeling salt diffusion in Iberian ham by applying MRI and data mining. *Journal of Food Engineering*, *189*, 115–122.

Caballero, D., Pérez-Palacios, T., Caro, A., Amigo, J. M., Dahl, A. B., ErsbØll, B. K., & Antequera, T. (2017). Prediction of pork quality parameters by applying fractals and data mining on MRI. *Food Research International*, *99*, 739–747.

Cabezas, L., Galán, E. & Fernández-Salguero, J. (2012). Relationships between physic-chemical and sensory characteristics of three types of dry-cured hams. *FleischWirtschaft International, 93 (2)*, 97-99.

Cáez-Ramírez, G., Alamilla-Beltrán, L., & Gutiérrez-López, G. F. (2017). Morphometric analysis and tissue structural continuity evaluation of senescence progression in fresh cut papaya (*Carica papaya* L.). *Journal of Food Engineering, 216*, 107-119.

Casillas, M. (1994). *Metodologías de caracterización de grasa de cerdo Ibérico para el control de calidad de sus productos*. Doctoral thesis. Córdoba: University of Córdoba. Spain.

Chen, Y., Wang, J., & Feng, J. (2017). Understanding the Fractal Dimensions of Urban Forms through Spatial Entropy. *Entropy*, *19*, 600.

De Bartolo, S.G., Gaudio, R., & Gabriele, S. (2004). Multifractal analysis of river networks: Sandbox approach. *Water Resource Research*, *40*, W02201.

Dómbradi, E., Timár, G., Bada, G., Cloetingh, S., & Horváth, F. (2007). Fractal dimension estimations of drainage network in the Carpathian-Pannonian system. *Global and Planetary Change, 58*, 197-213.

Dziuba, J., Babuchowski, A., Smoczynski, M., & Smietana, Z. (1999). Fractal analysis of caseinate structure. *International Dairy Journal, 9*, 287-292.

Fathi, M., Mohebbi, M., & Razavi, S. M. A. (2009). Application of image analysis and artificial neural network to predict mass transfer kinetics and color changes of osmotically dehydrated kiwifruit. *Food and Bioprocess Technology, 4(8),* 1357-1366.

Fernández, A., de Pedro, E., Núñez, N., Silio, L., García-Casco, J., & Rodríguez, C. (2003). Genetic parameters for meat and fat quality and carcass composition traits in Iberian pigs. *Meat Science, 64*, 405-410.

Fernandez, X., Monin, G., Talmant, A., Mourot, J., & Lebret, B. (1999). Influence of intramuscular fat content on the quality of pig meat - 1. Composition of the lipid fraction and sensory characteristics of m. longissimus lumborum. *Meat Science, 53*, 59-65.

García, J. (2002). *Clasificación y autentificación de canales de cerdo ibérico mediante espectroscopía en el infrarrojo cercano (NIRS)*. Doctoral thesis. Córdoba: University of Córdoba. Spain.

García-Armenta, E., Téllez-Medina, D. I., Sánchez-Segura, L., Alamilla-Beltrán, L., Hernández-Sánchez, H., & Gutiérrez-López, G. F. (2016). Multifractal breakage pattern of tortilla chips as related to moisture content. *Journal of Food Engineering, 168*, 96-104.

González-Martín, I., González-Pérez, C., Hernández-Méndez, J., Marqués-Macías, E., & Sanz-Poveda, F. (1999). Use of isotope analysis to characterize meat from Iberian breed swine. *Meat Science, 52*,437-441.

González-Martín, I., Pérez-Pavón, J. L., González-Pérez, C., Hernández-Méndez, J., & Álvarez-García, N. (2000). Differentiation of products derived from Iberian breed swine by electronic olfactometry (electronic nose). *Analytica Chimica Acta, 424*,279-287.

Grassberger, P. (1983). Generalized dimensions of strange attractors. *Physics Letter A, 97*, 227-230.

Grassberger, P., & Procaccia, I. (1983). Measuring the strangeness of strange attractors. *Physica D, 9*, 189-208.

Halsey, T. C., Jensen, M. H., Kadanoff, L. P., Procaccia, I., & Shraiman, B. I. (1986). Fractal measures and their singularities: The characterization of strange sets. *Physical Review A*, *33*, 1141-1151.

Hutchings, J. B., Luo, R., & Ji, W. (2002). Calibrated colour imaging analysis of food. In D. MacDougall (Ed.), *Colour in food* (pp. 352-366). Cambridge: Woodhead Publishing.ASA.

Jung, H., Yoon, W. B. (2017). Multifractal approaches of the ring tensile rupture patterns of dried laver (*Porphyra*) as affected by the relative humidity. *Journal of Food Science, 82 (12)*, 2894-2900.

Kaya, A., Ko, S., & Gunasekaran, S. (2008). Viscosity and color change during in situ solidification of grape pekmez. *Food and Bioprocess Technology, 4(2)*, 241-246

Kumar, M., & Mittal, G. S. (2010). Rapid detection of microorganisms using of soil image processing parameters and neural network. *Food and Bioprocess Technology, 3(5)*, 741-751.

Liu, M., Wang, M., Wang, J., & Li, D. (2013). Comparison of random forest, support vector machine and back propagation neural network for electronic tongue data classification: Application to the recognition of orange beverage and Chinese vinegar. *Sensors and Actuators B: Chemical*, *177*, 970–980.

Mandelbrot, B. B. (1982). *The fractal geometry of nature*. San Francisco: Freeman.

Mendoza, F., Valous, N., Delgado, A., & Sun, D.-W. (2011). Multifractal characterization of apple pore and ham fat-connective tissue size distributions using image analysis. In J. M. Aguilera, R. Simpson, J. Welti-Chanes, D. Bermudez-Aguirre, & G.

Barbosa-Canovas (Eds.), *Food Engineering Interfaces* (pp. 599-616). New York: Springer.

Mendoza, F., Valous, N. A., Sun, D.-W., & Allen, P. (2009). Characterization of fat-connective tissue size distribution in pre-sliced pork hams using multifractal analysis. *Meat Science*, *83*(4), 713–722.

Mendoza, F., Verboven, P., Ho, Q.T., Kerckhofs, G., Wevers, M., & Nicolaï, B. (2010). Multifractal properties of pore-size distribution in apple tissue using X-ray imaging. *Journal of Food Engineering, 99*, 206-215.

Morcuende, D., Estévez, M., Ramírez, M. R., de Alba, C., & Cava, R. (2003). Efecto de la línea materna y paterna en el cruce ibérico × duroc sobre los parámetros productivos y calidad de carne del pernil fresco. *II World Congress of Dry Cured Ham*. Cáceres, Spain.

Pérez-Palacios, T., Caballero, D., Antequera, T., Durán, M. L., Ávila, M., & Caro, A. (2017). Optimization of MRI Acquisition and Texture Analysis to Predict Physico-chemical Parameters of Loins by Data Mining. *Food and Bioprocess Technology*, *10*(4), 750–758.

Pérez-Palacios, T., Caballero, D., Caro, A., Rodríguez, P. G., & Antequera, T. (2014). Applying data mining and Computer Vision Techniques to MRI to estimate quality traits in Iberian hams. *Journal of Food Engineering*, *131*, 82–88.

Press, W.H., Teukolsky, S.A., Vetterling, W.T., & Flannery, B.P. (1996). *Numerical Recipes in Fortran 90: The Art of Parallel Scientific Computing*, Cambridge: Cambridge University Press (Volume 2).

Real Decreto 4/2014, de 10 de enero, por el que se aprueba la norma de calidad para la carne, el jamón, la paleta y la caña de lomo ibérico. Spanish Ministry of Agriculture, Food and Environment.

Romano, A., Masi, P., & Cavella, S. (2018). Visual evaluation of sliced Italian salami by image analysis. *Food Science & Nutrition, 6*, 153-159.

Ropodi, A. I., Panagou, E. Z., & Nychas, G.-J. E. (2016). Data mining derived from food analyses using non-invasive/non-destructive analytical techniques; determination of food authenticity, quality & safety in tandem with computer science disciplines. *Trends in Food Science & Technology*, *50*, 11–25.

Ruiz, J., & Petrón, M.J. (2000). Métodos para la clasificación de la materia prima. In J. Ventanas (Ed.), *Tecnología del jamón Ibérico. De los sistemas tradicionales a la* *explotación racional del sabor y el aroma.* (pp. 131-160). Madrid: Ediciones Mundi-Prensa.

Santos Pereira, L. F., Barbon, S., Valous, N. A., & Barbin, D. F. (2018). Predicting the ripening of papaya fruit with digital imaging and random forests. *Computers and Electronics in Agriculture*, *145*, 76–82.

Serrano, S., Perán, F., Jiménez-Hornero, F. J. & Gutiérrez de Ravé, E. (2013). Multifractal analysis application to the characterization of fatty infiltration in Iberian and White pork sirloins. *Meat Science, 93*, 723-732.

Tejada, J.F., Gandemer, G., & Antequera, T. (2002). Lipid traits of muscles as related to genotype and fattening diet in Iberian pigs: total intramuscular lipids and triacylglycerols. *Meat Science, 60*, 357-363.

Tél, T., Fülöp, Á., & Vicsek, T. (1989). Determination of fractal dimensions for geometrical multifractals. *Physica A, 159*, 155-166.

Valous, N.A., Mendoza, F., Sun, D-W., & Allen, P. (2009a). Colour calibration of a laboratory computer vision system for quality evaluation of pre-sliced hams. *Meat Science, 81*, 132-141.

Valous, N. A., Mendoza, F., Sun, D.-W., & Allen, P. (2009b). Texture appearance characterization of pre-sliced pork ham images using fractal metrics: Fourier analysis dimension and lacunarity. Food Research International, 42(3), 353–362.

Valous, N. A., Zheng, L., Sun, D.-W., & Tan, J. (2016). Quality Evaluation of Meat Cuts. In Computer Vision Technology for Food Quality Evaluation (pp. 175–193). Elsevier.

Ventanas, J. (2008). *El jamón Ibérico: de la dehesa al paladar*. Madrid: Ediciones Mundi-Prensa.

Vicsek, T. (1990). Mass multifractals. *Physica A, 168*, 490-497.

Vicsek, T., Family, F., & Meakin, P. (1990). Multifractal geometry of diffusion-limited aggregates. Europhysics Letter, 12, 217-222.

Zheng, C., Sun, D. W., & Zheng, L. (2006). Recent developments and applications of image features for food quality evaluation and inspection – A review. *Trends in Food Science and Technology, 17*, 642–655.R

Figure captions

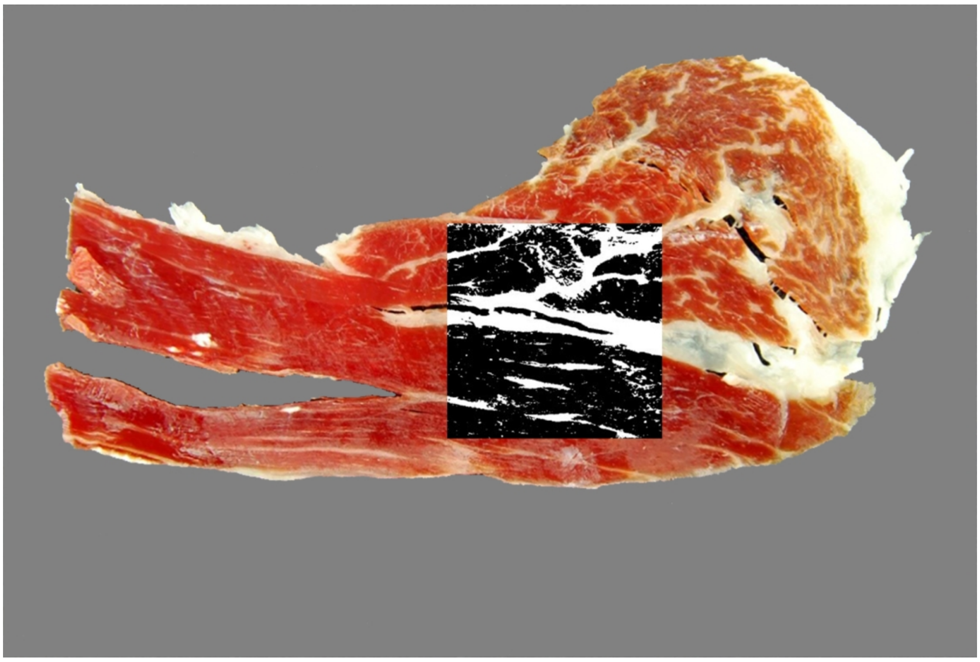

Fig. 1. Original image of Iberian ham sample and selected ROI (512x512 pixel). Black and white pixels stand for fatty infiltration and lean meat, respectively.

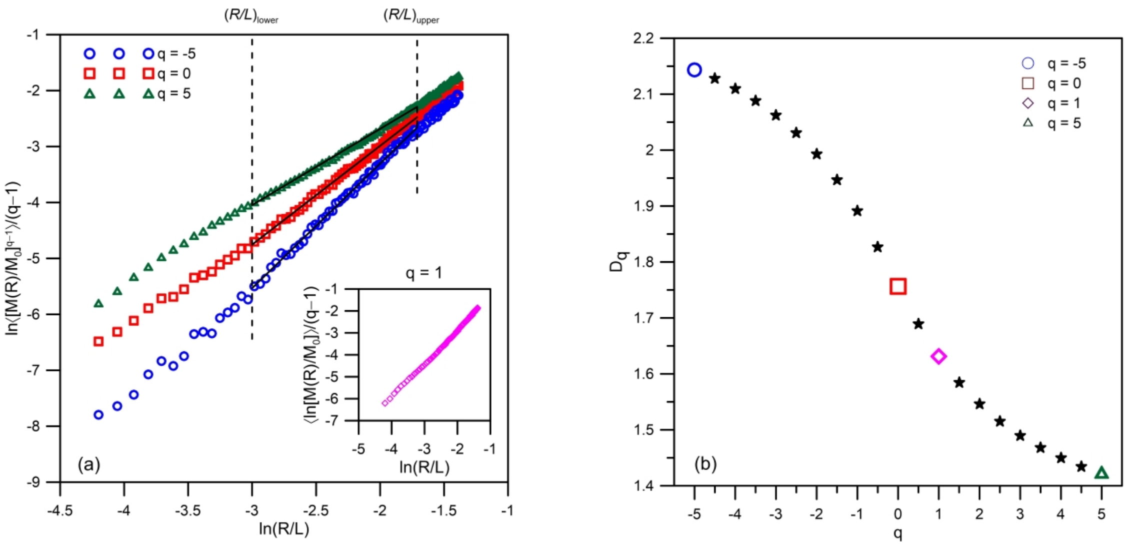

Fig. 2. Some results derived from multifractal sandbox method: (a) Scaling curves for q = -5, 0, 1, 5 with $(R/L)_{lower}$ and $(R/L)_{upper}$ as the low and high limits for the linear fits whose slopes determine fractal dimensions D_{-5}, D_0, D_1 and D_5. (b) Generalized fractal dimensions spectrum where the locations of the previously mentioned fractal dimensions are indicated by the corresponding color symbols.

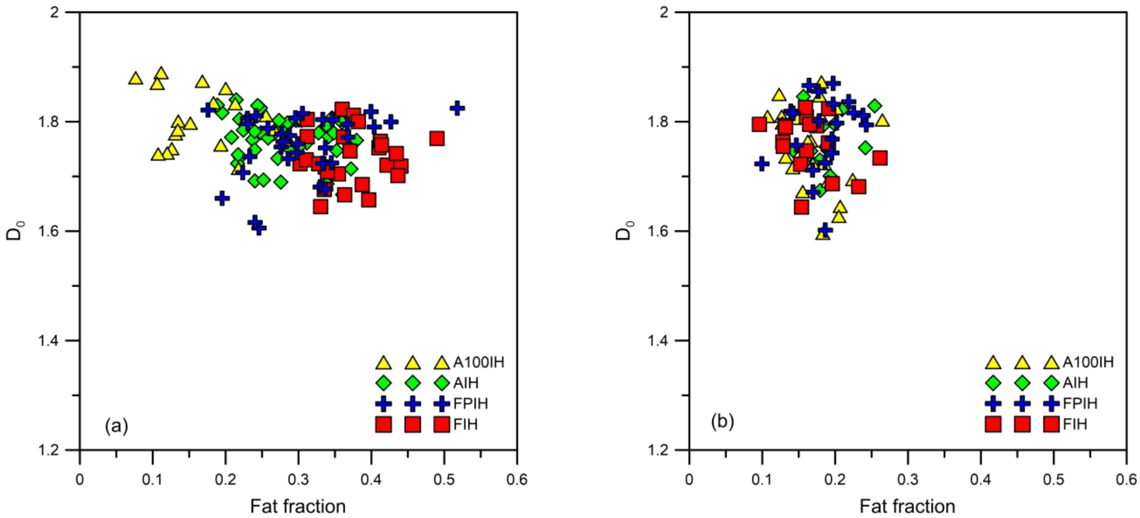

Fig. 3. Scatter plots depicting the relationships between the box-counting dimension (or fractal dimension), D_0, and fat fraction found for each ham designation when (a) knife and (b) slicer cutting are used.

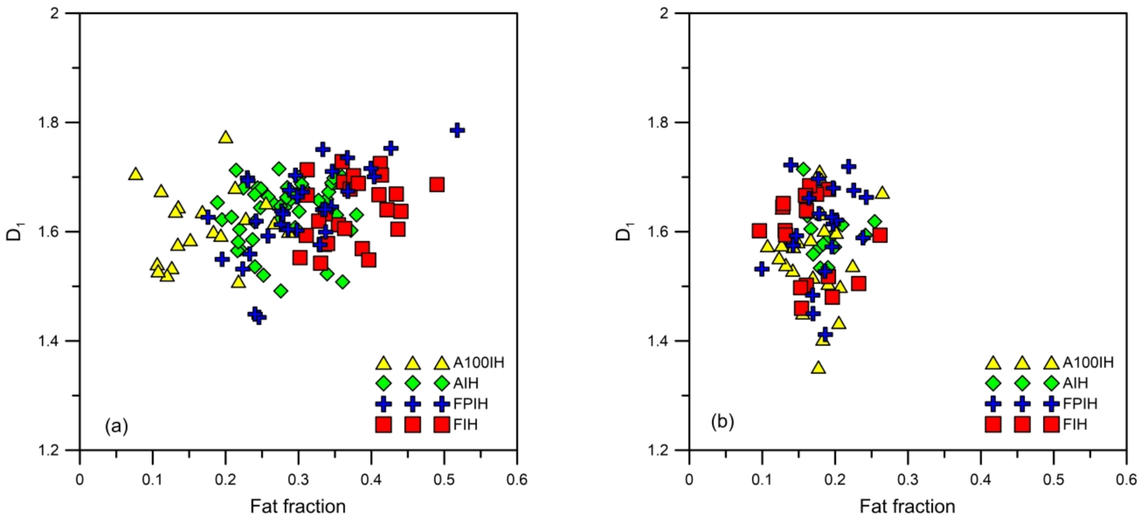

Fig. 4. Scatter plots showing the associations between the information or entropy dimension, D_1, and fat fraction got for each ham designation when (a) knife and (b) slicer cutting are used.

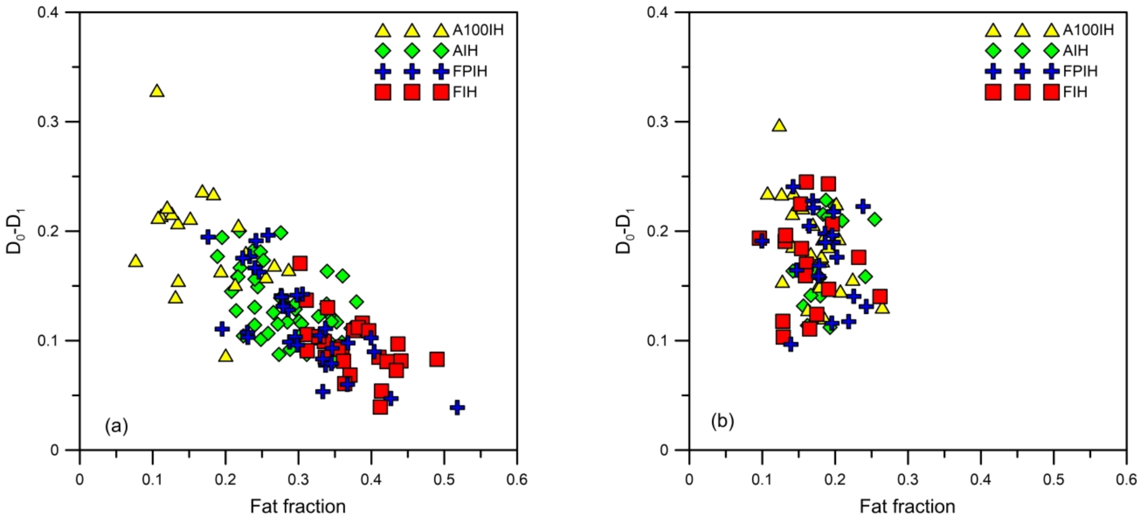

Fig. 5. Scatter plots describing the links between the multifractal dimension increment, D_0 - D_1 , and fat fraction yielded for each ham designation when (a) knife and (b) slicer cutting are used.

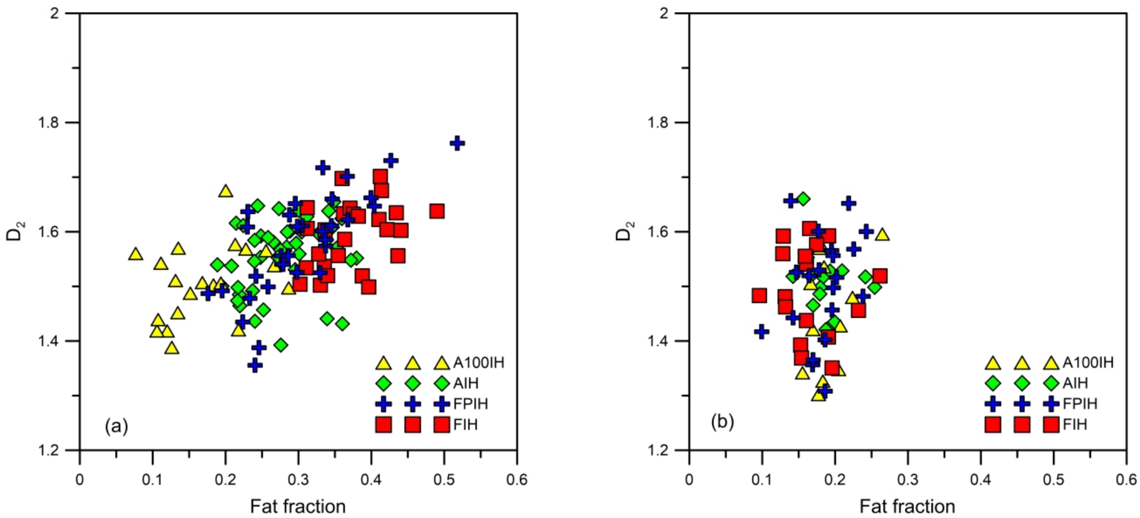

Fig. 6. Scatter plots illustrating the relationships between the correlation dimension, D_2, and fat fraction obtained for each ham designation when (a) knife and (b) slicer cutting are used.

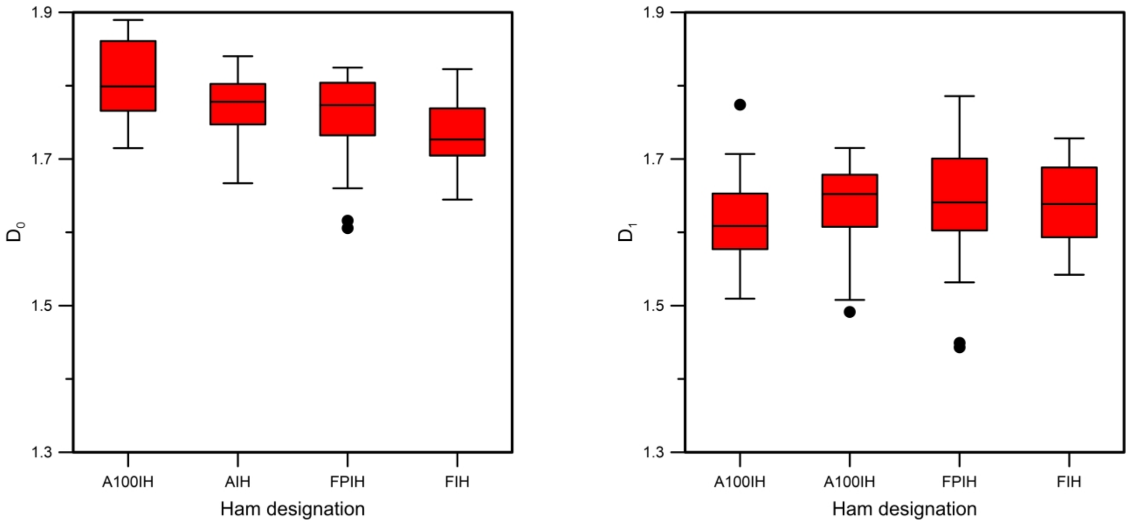

Fig. 7. Box and whisker plots corresponding to D_0 and D_1 fractal dimensions obtained for each ham designation from samples cut with knife. Black dots represent the outliers obtained by considering an interquartile range affected by a factor of 1.5.

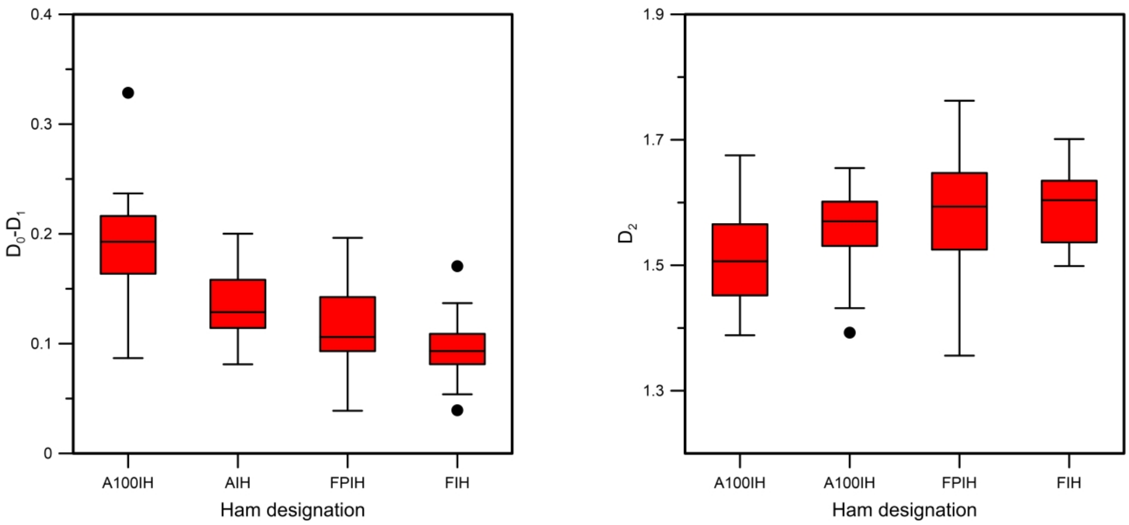

Fig. 8. Box and whisker plots corresponding to D_0 - D_1 and D_2 fractal dimension obtained for each ham designation from samples cut with knife. Black dots represent the outliers obtained by considering an interquartile range affected by a factor of 1.5.

Tables

Table 1. Mean and standard error for fat, moisture and water activity in the four designations of Iberian ham.

	a_w		Fat (%)		Moisture (%)	
Designation	Mean	Standard error	Mean	Standard error	Mean	Standard error
A100IH	0.823	0.00887	26.10	3.77625	35.09	1.71296
AIH	0.830	0.01213	31.41	3.95989	33.42	2.60812
FPIH	0.857	0.01285	33.80	6.49552	36.93	3.91204
FIH	0.865	0.01292	35.26	6.49400	37.16	2.77758

Table 2. Mean and standard error for the considered fractal dimensions in the four designations of Iberian ham when knife cutting is used.

	Fractal dimension					
	D_0		D_1		D_2	
Ham designation	Mean	Standard error	Mean	Standard error	Mean	Standard error
A100IH	1.804	0,05180	1.612	0,06791	1.508	0,06791
AIH	1.769	0,04175	1.636	0,04065	1.557	0,06506
FPIH	1.758	0,05854	1.641	0,07989	1.579	0,09495
FIH	1.734	0,04778	1.640	0,05777	1.594	0,06016

Table 3. Mean and standard error for the considered fractal dimensions in the four designations of Iberian ham when slicer cutting is used.

	Fractal dimension					
	D_0		D_1		D_2	
Ham designation	Mean	Standard error	Mean	Standard error	Mean	Standard error
A100IH	1,757	0,07674	1,570	0,08100	1,452	0,07521
AIH	1,754	0,04336	1,579	0,03242	1,493	0,04196
FPIH	1,790	0,05572	1,612	0,07649	1,511	0,08839
FIH	1,760	0,05229	1,587	0,07737	1,493	0,08269

Highlights

Fat infiltration in Iberian ham exhibits multifractal nature
A set of multifractal dimensions describe fat tissue distribution in ham cut by knife
Multifractal dimensions could be used as features in ham quality prediction